Proceedings of the 20th International Conference on Soil Mechanics and Geotechnical Engineering– Rahman and Jaksa (Eds)

Investigation of the deformation mechanism and the stability of deformable body in the reservoir area based on the D-InSAR monitoring

Enquête sur le mécanisme de déformation et la stabilité du corps déformable dans la zone du réservoir sur la base de la surveillance D-InSAR

Yujie Wang, Long Jiang, Ping Sun, Xinchao Lin
Department of Geotechnical Engineering, China Institute of Water Resources and Hydropower Research, Beijing, China

ABSTRACT: Differential Interferometric Synthetic Aperture Radar (D-InSAR) technology is a regional ground deformation remote sensing monitoring technology developed in recent years. It has the characteristics of the wide monitoring range, the high spatial resolution, the high measurement accuracy, all-day and all-weather monitoring. This paper firstly applies the D-InSAR monitoring technology to study the deformation failure mechanism of the left bank of the Alagou reservoir area and the stability of the deformable body is evaluated on this basis. The research results show that the D-InSAR technology can be used for the landslide deformation analysis. When the SAR image reaches 30 or more, the data analysis accuracy can reach mm level, which can provide an effective way for the global identification, the pre-deformation evolution, the prediction and the evaluation of the reservoir bank landslides. The results also indicate that the deformation trend of the deformable body on the left bank is consistent with the fluctuation of the water level. The overall performance is that the micro-deformation gradually penetrates from the upstream side until the overall deformation and the subsidence are coordinated, and the boundary of the micro-deformation area can be accurately identified. Besides, the deformable body on the left bank is a traction landslide with poor overall stability, and the main cause is the fluctuation of the reservoir water level. Furthermore, after the implementation of the emergency treatment for the deformable body, the overall deformation of the deformable body does not continue to develop and the growth rate is relatively low, and the deformable body is still in the process of the adjustment of the new stress equilibrium. Lastly, based on the D-InSAR technology and the rigid body limit equilibrium method, a set of systematic analysis methods of the slope deformation evolution, the formation mechanism and the stability evaluation are proposed to provide some experience and reference for other similar slope engineering treatment.

RÉSUMÉ : La technologie du radar interférométrique à synthèse d'ouverture différentielle (D-InSAR) est une technologie régionale de surveillance à distance de la déformation du sol développée ces dernières années. Il présente les caractéristiques d'une large plage de surveillance, d'une résolution spatiale élevée, d'une précision de mesure élevée, d'une surveillance toute la journée et par tous les temps. Cet article applique tout d'abord la technologie de surveillance D-InSAR pour étudier le mécanisme de rupture par déformation de la rive gauche de la zone du réservoir d'Alagou et la stabilité du corps déformable est évaluée sur cette base. Les résultats de la recherche montrent que la technologie D-InSAR peut être utilisée pour l'analyse de la déformation des glissements de terrain. Lorsque l'image SAR atteint 30 ou plus, la précision de l'analyse des données peut atteindre le niveau du mm, ce qui peut fournir un moyen efficace pour l'identification globale, l'évolution de la pré-déformation, la prédiction et l'évaluation des glissements de terrain du réservoir. Les résultats indiquent également que la tendance à la déformation du corps déformable en rive gauche est cohérente avec la fluctuation du niveau d'eau. La performance globale est que la micro-déformation pénètre progressivement du côté amont jusqu'à ce que la déformation globale et la subsidence soient coordonnées, et que la limite de la zone de micro-déformation puisse être identifiée avec précision. Par ailleurs, le corps déformable en rive gauche est un glissement de terrain de traction avec une mauvaise stabilité globale, et la cause principale est la fluctuation du niveau d'eau du réservoir. De plus, après la mise en œuvre du traitement d'urgence pour le corps déformable, la déformation globale du corps déformable ne continue pas à se développer et le taux de croissance est relativement faible, et le corps déformable est toujours en cours d'ajustement de la nouvelle contrainte. équilibre. Enfin, sur la base de la technologie D-InSAR et de la méthode d'équilibre limite des corps rigides, un ensemble de méthodes d'analyse systématique de l'évolution de la déformation des pentes, du mécanisme de formation et de l'évaluation de la stabilité sont proposés pour fournir une expérience et une référence pour d'autres traitements similaires d'ingénierie des pentes. .

KEYWORDS: Alagou reservoir; Deformable body of reservoir area; D-InSAR technology; Rigid body limit equilibrium method

1 INTRODUCTION.

Water conservancy and hydropower projects of high dams and large reservoirs are emerging one after another, and the reservoir bank reconstructions (reservoir bank landslides) occur from time to time. At this stage, the occurrence, the development and the disaster of landslides from time to time exceed the scope of the investigation and the evaluation of the existing landslides and the expected dangerous areas. The existing monitoring methods such as GPS, the inclinometer, the three-dimensional laser scanning, and the micro-deformation radar can only obtain the displacement information of the designated landslide, but it is difficult to obtain the ground displacement information of a wider range (Blanco-Sànchez et al. 2008).

Differential Interferometric Synthetic Aperture Radar (D-InSAR) is a regional ground deformation remote sensing monitoring technology that has been widely developed in recent years. It has the characteristics of the wide monitoring range, the high spatial resolution, the good measurement accuracy and all-time and all-weather monitoring, which can provide an effective approach for the global identification, the pre-deformation evolution, the prediction and the evaluation of landslides (Herrera et al. 2013). Gabriel et al. (1989) applied the D-InSAR technology to the ground deformation monitoring of the Imperial Valley irrigation area for the first time, and demonstrated the feasibility of the D-InSAR technology and the achievement of the measurement accuracy reaching the cm level. Achache et al. (1995) carried out the displacement monitoring of the landslide and obtained 6 interference fringe patterns. They compared with the accuracy of the traditional ground monitoring methods and verified that the accuracy of the technology to monitor the landslide deformation satisfied the practical engineering requirements. Squarzoni et al. (2003) further conducted landslide deformation monitoring and obtained 15 interference fringe patterns, and deduced the evolution law of the deformation at

different displacement rates. Colesanti et al. (2003) coupled the SAR data and the PS technology to improve the monitoring accuracy of the D-InSAR technology to the mm level and carried out the ground displacement monitoring. Xia et al. (2004) utilized the D-InSAR technology and the PS technology to conduct special monitoring of the Xintan landslide and the Lianziya landslide in the Three Gorges reservoir area. Zhang et al. (2010) adopted the D-InSAR technology to monitor the Sichuan Jiaju landslide and obtained the two-phase displacement of the landslide. Huang et al. (2011) and Wang et al. (2010) have numerously investigated the application of the D-InSAR technology to the landslide monitoring in alpine valley reservoir area with plenty of useful research results. Wang (2010) used 40 SAR images to monitor the deformation of the landslide in Badong New City Area and obtained the deformation evolution law in different time periods. Shi et al. (2017) used the D-InSAR technology to monitor the deformation of the Shuping landslide in the Three Gorges Reservoir area, and found that periodic changes in the reservoir water level would affect the landslide deformation. Zhang et al. (2018) applied the D-InSAR technology to study the early identification of landslides in the Bailong River Basin and successfully identified 133 active slopes. Wang et al. (2015) conducted an error analysis on the application of the D-InSAR technology in alpine and canyon region, and proposed a dynamic monitoring method for landslides based on the D-InSAR technology. Zhao et al. (2018) conducted the deformation monitoring on the Jinpingzi landslide and found that there are spatial differences in the deformation of the landslide, and reservoir water level fluctuations and rainfall are the main inducing factors for the landslide.

In summary, the measurement accuracy of the D-InSAR technology in monitoring ground deformation has gradually developed from cm level to mm level or even sub-mm level. The effect is remarkable in engineering application such as the recognition of landslide area, the deformation evolution law and the sensitivity factors, but the research on the formation mechanism, the stability analysis and the evaluation of landslides are comparatively limited. Therefore, the identification and the evaluation system of the deformable body in the reservoir area based on the D-InSAR monitoring has been established, and the influence range of the reservoir deformation, the deformation evolution law, the causes and the development of landslides, and the inversion of stability parameters are investigated. The results can provide a technical support for the analysis and the evaluation of the landslide stability, and also provide a scientific basis for the prediction, the evaluation, and the prevention of landslide disasters in potential dangerous areas in similar reservoir areas.

2 ENGINEERING GEOLOGICAL CONDITIONS OF THE DEFORMABLE BODY ON THE LEFT BANK OF ALAGOU RESERVOIR

2.1 *Overview of the deformable body project on the left bank*

The topographic and geomorphological characteristics of the deformable body on the left bank are shown in Figure 1. The construction of the project started in April 2011, and the reservoir was officially impounded in November 2014. The water level reached 935m~940m elevation from October 2015 to April 2016, and briefly dropped to 921m from May to June 2016. From July to August, it restored to the highest elevation of 942.0m, which was close to the normal storage level of 944.5m. In the process of water release from September to mid-October 2016, it was found that the left bank slope began to deform. In the following two years, the reservoir water level was mainly maintained at an elevation of 916m to 932m, and the deformation of the left bank continued to collapse, and the slope deformation increased significantly.

Figure 1. The geographic location of the deformable body on the left bank

2.2 *The boundary conditions of the deformable body on the left bank*

According to the field survey of the deformable body on the left bank of the reservoir area, it is found that the upstream of the deformable body is bounded with the gentle inclined structural plane (Figure 2, a), and there are multiple groups of gentle inclined structural planes with the occurrence of N60°W·NE∠43°. The downstream boundary is the fault F1 (Figure 2, b), where the fault gouge and the landslide scratches are obviously exposed. The landslide scratch is 140° and the fault occurrence is N41ºW·SW∠53º. The bottom boundary is a near-horizontal joint fracture zone (Figure 2, c). The joint plane J3 with low inclined angle is developed with the appearance of N85°W·SW∠15°, and the elevation is about 920m. The bank edge is dominated by tensile cracks with a staggered distance of about 5m. The tensile cracks in the local disintegration area of the deformable body on the left bank and in the inner slope tend to be between 180° and 190° (Figure 2, d).

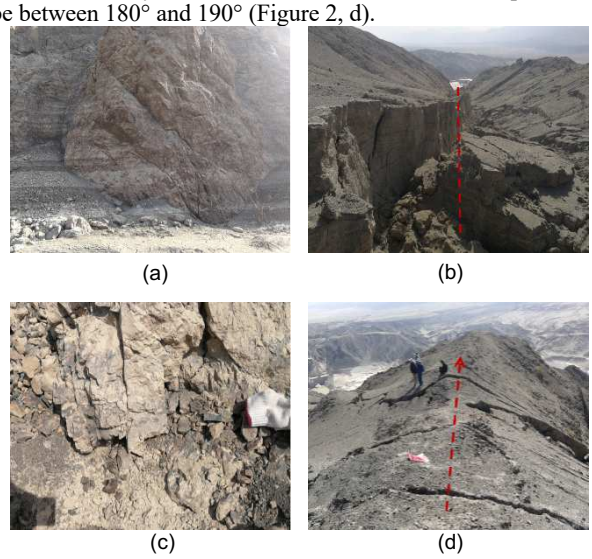

Figure 2. Reconnaissance maps of the deformable body on the left bank: (a) upstream side gently inclined structural plane, (b) downstream fault, (c) front joint zone, (d) local disintegration tensile cracks.

2.3 *Evolution of the large deformation of the deformable body on the left bank*

The satellite image of DEM is used to calculate the accumulated large deformation of the deformable body on the left bank. The inherent attributes of the permanent scatterers are used to match between two or more images to calculate the deformation of the permanent scatterers. The distribution of typical points of the accumulated large deformation is shown in Figure 3.

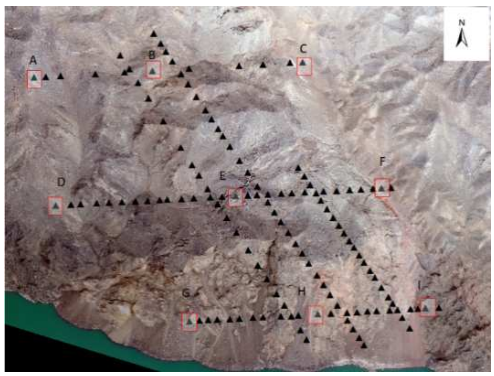

Figure 3. Distribution map of typical measuring points of deformable body.

It can be seen from the deformation and the deformation rate of the typical measuring points of the deformable body (Figure 4 and Figure 5) that the deformation of the deformable body is relatively consistent with the change of the reservoir water level, and the deformation rate has been fluctuating between 0 and 1.06 mm/d with an average of 0.44 mm/d. In the initial stage of the water storage, the deformation is small with slight increase. When the water level of the reservoir rises to 920m for the first time, the small deformation begins to appear, and after it rises to 940m again the large deformation begins to appear. Later, when the reservoir water level drops to 920m or rises to 940m again, the deformation continues to develop, and it is consistent with the fluctuation of the reservoir water level. The deformation of the middle part E and the lower part H of the deformable body alternately increases with the change of the reservoir water level and time, which is relatively equivalent in overall. It is about 4.4m before the treatment and the deformation of the upper part B of the deformable body occurs earlier than the middle and lower parts, but only with small magnitude increases which is about 2.3m before the treatment.

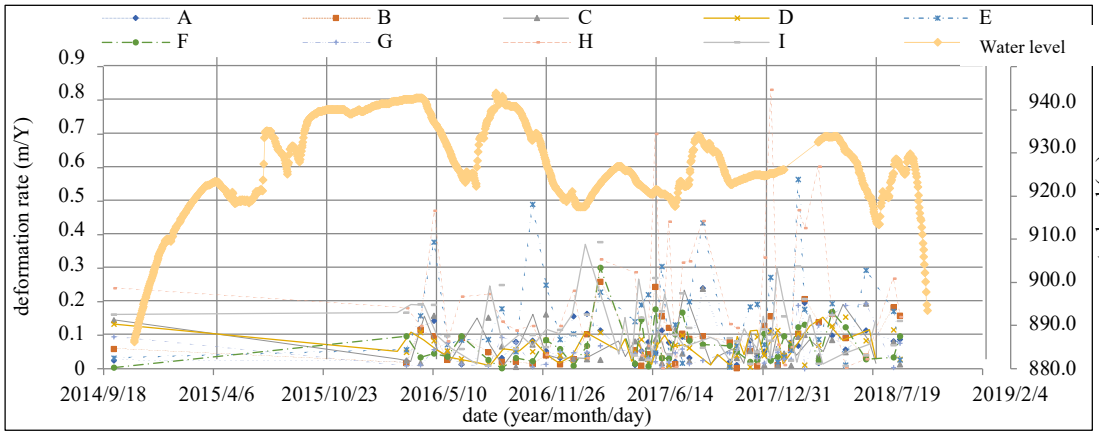

Figure 4. Directional deformation of the typical measuring points of the deformable body on the left bank

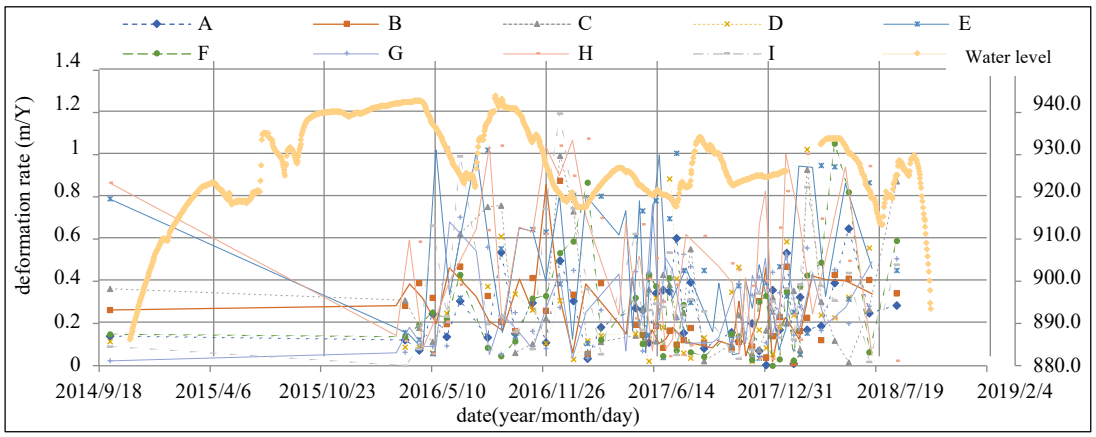

Figure 5. Positional deformation of the typical measuring points of the deformable body on the left bank

3 D-INSAR MONITORING RESULTS AND THE DEFORMATION MECHANISM OF THE DEFORMABLE BODY ON THE LEFT BANK

3.1 *The basic principle and the accuracy of D-InSAR*

Since October 2014, a total of 44 and 55 remote sensing data scenes in ascending and descending orbit have been collected in this region, respectively. Through the calculation and the analysis, the number of remote sensing data scenes in this area is more than 30, and the ground deformation accuracy reaches mm level, which meets the technical requirements of the deformation evolution law analysis of the deformable body in the reservoir area.

3.2 *Slight deformation of the deformable body on the left bank of the reservoir area*

The deformation evolution trend of the deformable body on the left bank during the impoundment period is shown in Figure 7. It is revealed that the red dot represents sinking (+), and the green dot indicates the zero deformation nearby area, and the blue dot denotes uplift (-), and the missing part specifies that the deformation exceeds the solution measurement, which belongs to the large deformation area. Before impoundment, the small deformation of the deformable body on the left bank occurred

near the downstream mountain with the small amount of change. When the water storage was about 933m, the deformable body on the left bank had a relatively obvious subsidence trend from local to overall. Until June 2016, the upper part of the upstream side and the lower part of the downstream side deformed significantly, and the micro-deformation gradually penetrated from the upstream side until the overall deformation and the subsidence were consistently coordinated.

Until August 2017, the deformable body on the left bank internally adjusted and the boundary of the micro-deformation area of the deformable body was basically determined after August 2017. Firstly, it shows that the area is already in the process of deformation before water storage, and the geological conditions are not conducive to the stability of the deformed body. Secondly, the deformation of the deformable body on the left bank has a certain hysteresis with the rise and fall of the reservoir water level. Thirdly, as the reservoir water level rises, the deformation of the deformable body on the left bank increases to a certain extent from the elevation of 922m to 928m of the reservoir water level which further softens the unfavorable structural planes to reduce the sliding resistance. Therefore, the unfavorable structural plane of the deformable body on the left bank may be below the elevation of 928m.

3.3 *The genetic mechanism of the deformable body on the left bank of the reservoir area*

The micro-deformation of the deformable body on the left bank is not significant before the water storage. From April 2015 to August 2015, the upstream side deformed significantly. From March 2016 to June 2016, the upper part of the upstream side and the lower part of the downstream side deformed considerably. The accumulated micro-deformation gradually penetrated from the upstream side until the overall deformation and the subsidence were consistent. After August 2017, the boundary of the micro-deformation area of the deformable body was basically stable.

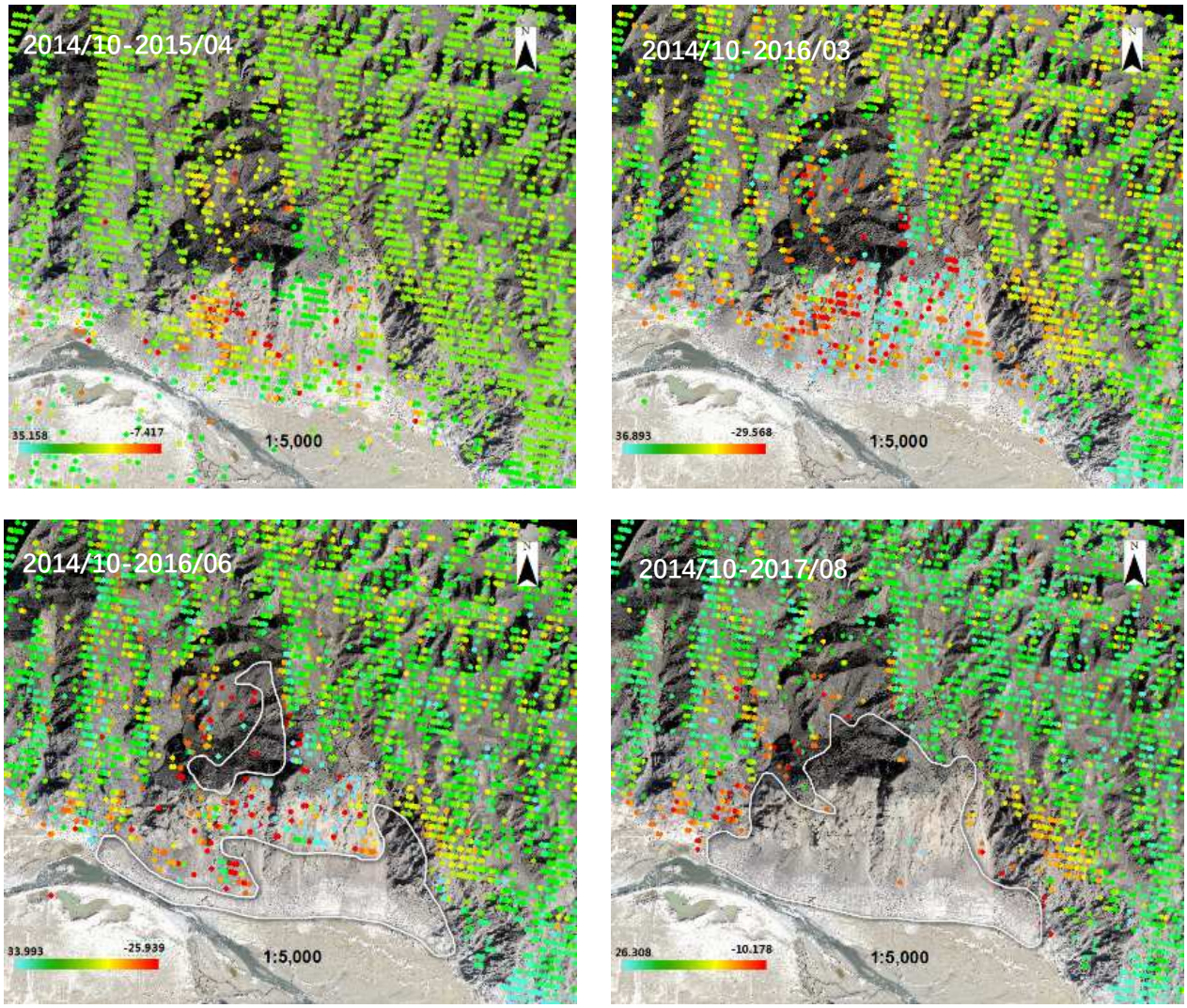

Figure 7. Cumulative micro-deformation during storage period of the deformable body on the left bank

The large deformation area of the deformable body on the left bank is consistent with the micro deformation boundary, and the deformation of the deformable body exists but not significant before impoundment. When the water level reaches 922m ~ 928m, the subsidence appears, and the increase is significant with the change of reservoir water level. During the impoundment process, the joint plane of the gently inclined crack with the elevation of about 920m at the front edge of the deformable body is softened, and the front edge of the deformable body slides towards the right bank to the upstream. Continuous cracks appear in the downstream fault and the rear edge of the deformable body, and the deformable body is even partially disintegrated which are controlled by the bottom sliding plane.

In summary, the deformable body on the left bank is a traction landslide, which is controlled by the sliding plane at the

bottom of the front edge of the deformable body.

4 TREATMENT AND STABILITY EVALUATION OF THE DEFORMABLE BODY ON THE LEFT BANK

4.1 *Stability of the deformable body on the left bank of the reservoir area*

According to the results of field survey, the D-InSAR and image tracking of the deformable body on the left bank, the recommended geological values are selected as shown in Table 1. The engineering geological division and the calculation sectional graph of the deformable body on the left bank are illustrated in Figure 8, and the calculation results are shown in Figure 9.

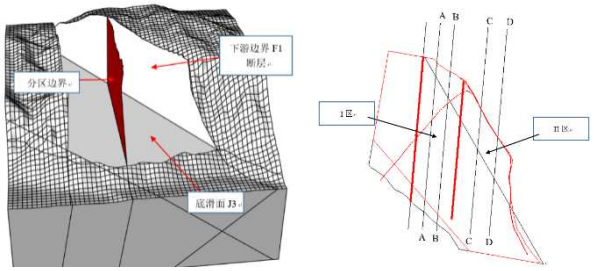

Figure 8. The engineering geological division of the deformable body on the left bank.

The safety factor of the overall anti-sliding stability in zone I is greater than 1.35 and that of the local sliding from the front edge is between 0.99 to 1.05, which indicating that the overall stability of the slope in this zone is reliable, but the local part of the front edge is basically in the critical state. The safety factor of the overall sliding in zone II is between 0.62 to 0.93 and that of the local sliding from the front edge is between 0.86 to 0.98, which signifying that the overall and the local stability of the slope in this zone is poor. The overall law of the calculation results of the anti-sliding stability of the deformable body on the left bank is relatively consistent with that of D-InSAR.

Table 1. Suggested geological values for the physical and mechanical parameters of the rock mass and structural planes of the deformed body on the left bank

Material types		Shear strength parameters				Volumetric weight
		Above the water level		below the water level		
		f	*c*/kPa	*f*	*c*/kPa	γ/kN/m^3
tuffaceous siltstone, tuffaceous sandstone, et al. (D3tb)	fully weathered	0.35~0.40	100.0	—	—	24.8~25.0
	strongly weathered	0.60~0.65	150.0~200.0	—	—	25.0~25.5
	slightly weathered	0.80~0.85	400.0~500.0	0.80	400.0	25.6~26.0
F1 fault		0.38~0.43	16.0~20.0	0.35~0.40	14.0~18.0	—
J1, J2, and J4 structural plane		0.42~0.45	20.0	0.38~0.40	0.0	—
J3 (slipping surface)		0.55	50.0	0.50	40.0	

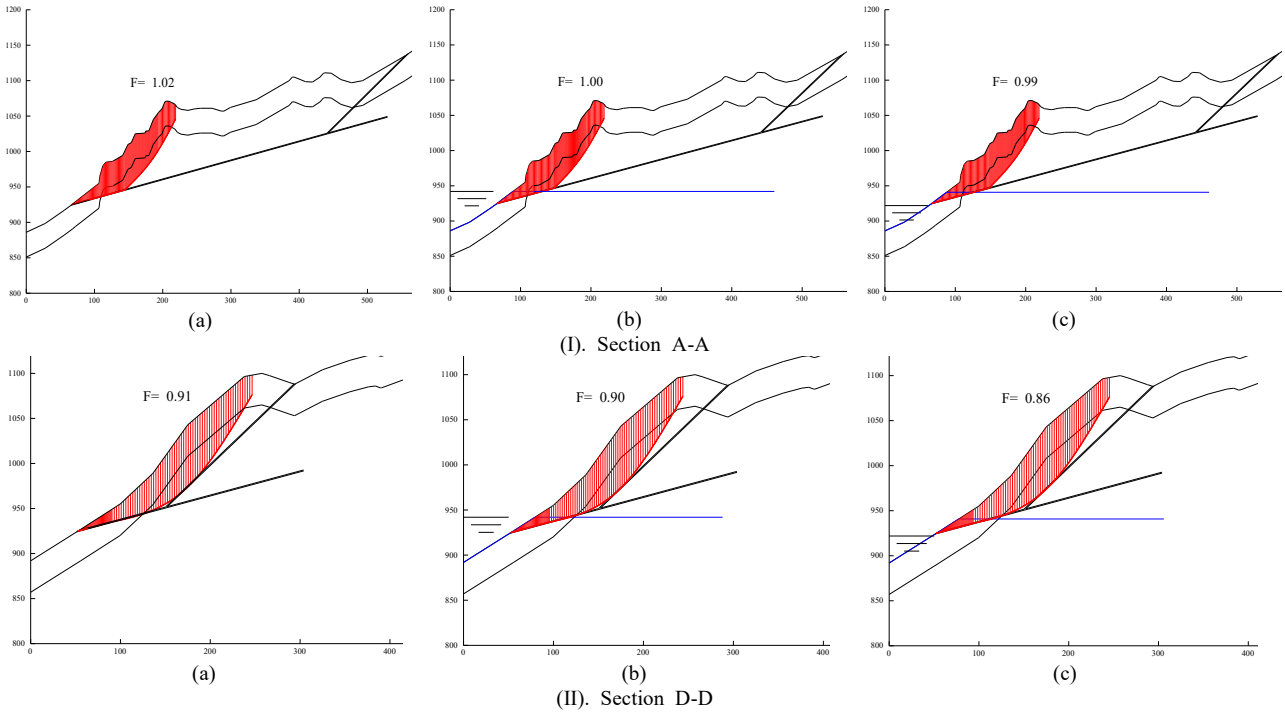

Figure 9. The calculation diagram of the anti-sliding stability of the typical section. (a) the natural slope of the water storage level; (b) the water storage level to 942.0m; (c) the sudden drop of the water level.

4.2 *Treatment of the pressure foot for slope-cutting and unloading of the deformable body on the left bank of the reservoir area*

In order to make this deformable body meet the requirements u nder various conditions of the normal operation of the reservoir, the slope cutting and the load reduction treatment is carried ou t, and the excavation waste is placed at the foot of the slope to f orm a natural resting slope to meet the stability requirements.

The slope treatment scheme is implemented in two steps. The first step is the emergency treatment which requires unloading to an elevation of 1080m. The second step is the comprehensive treatment which requires unloading to an elevation of 1000m. After the implementation of the two steps, the safety factor of the slope stability under the normal water level conditions reached 1.08, and the safety factor under 930m water level conditions reached 1.1, which has a certain safety margin.

4.3 *Evaluation of the treatment effect of the deformable body on the left bank of the reservoir area*

The deformation of the deformable body on the left bank has been increasing since the occurrence of the large deformation.

As the treatment of the pressure foot for slope-cutting and unloading of the deformable body is implemented, the internal stress of the deformable body has been adjusted. Although the deformation has been increasing, the growth rate has fluctuated greatly. After the first step of the treatment is implemented, the reservoir begins to operate at the low water level. The deformation does not continue to develop and the growth rate remain low. The deformable body is still in the process of micro-adjustment of the new stress equilibrium, thus the monitoring should be strengthened to provide a dynamic support for the low water level operation of the reservoir and the basic data for the next comprehensive treatment of the deformable body.

5 CONCLUSIONS

Based on the differential interferometry synthetic aperture radar (D-InSAR) technology, the deformation influence range, the deformation evolution law, the landslide occurrence and the development causes, the disaster rules and the stability of the reservoir area have been investigated and a series of useful conclusions have been obtained for the reference of other similar cases.

- D-InSAR technology can be used to monitor bank landslides. The SAR image can reach more than 30 pieces and the accuracy can reach mm level. It can provide an effective approach for investigating the global identification, the early deformation evolution, the prediction and the evaluation of the bank landslides.
- The micro-deformation of the deformable body on the left bank reveals that the micro-deformation gradually penetrates from the upstream side until the overall deformation and the subsidence are consistent, and the boundary of the micro-deformation area can be accurately distinguished. The deformable body on the left bank is a traction landslide which is controlled by the bottom sliding plane of the front edge of the deformable body. Its own geological conditions are not conducive to the stability of the deformable body, and the fluctuation of the reservoir water level is the main inducing factor.
- The overall stability of the deformable body on the left bank is relatively poor, and the overall law of the anti-sliding stability is consistent with the monitoring results of the D-InSAR. After the implementation of emergency treatment for the deformable body, the overall deformation does not continue to develop and the growth rate is relatively low. The deformable body is still in the process of micro-adjustment of the new stress equilibrium, so the monitoring should be strengthened to provide a dynamic support for the low water level operation of the reservoir.
- Based on the D-InSAR technology and the rigid body limit equilibrium method, a set of systematic analysis methods of the slope deformation evolution, the formation mechanism and the stability evaluation are proposed to provide some experience and reference for other similar slope engineering treatment.

6 REFERENCES

Achache J, Fruneau B, Delacourt C. Applicability of SAR interferometry for operational monitoring of landslides[C]//Proceedings of the Second RES Applications Workshop. London,6-8 December 1995:165-168.

Blanco-Sànchez P, Mallorquí J J, Duque S, et al. The Coherent Pixels Technique (CPT): An Advanced DIn SAR Technique for Nonlinear Deformation Monitoring [M]. Earth Sciences and Mathematics. Birkhäuser Basel,2008.

Colesanti F, Ferretti A, Pratic,Rocca F. Monitoring Landslides and tectonic motions with the Permanent Scatterers Technique[J]. Engineering Geology,2003,68(1-2): 3-14.

Gabriel A.K., R.M.Goldstein, H.A.Zebker, Mapping Small Elevation Changes OVER Large Areas: Differential Radar Interferometry[J].Geophys.Res.,1989,94(B7):9183-9191.

Herrera G, Gutiérrez F, García-Davalillo J C, et al. Multi-sensor advanced DIn SAR monitoring of very slow landslides: The Tena Valley case study (Central Spanish Pyrenees) [J]. Remote Sensing of Environment, 2013, 128(1):31-43.

Huang J H，Xie M W，Ma R, et al. Design of the arctifical corn er reflector in interferometric synthetic aperture radar and reco g n i t i o n i n i m a g e s [J]. Journal of Geomatics Science and Technology，2011，(04)：270-273.

Shi X., Jiang H., Zhang L., et al.. Landslide displacement monitoring with split-bandwidth interferometry: A case study of the shuping landslide in the three gorges area[J]. Remote Sensing, 2017, 9(9):937.

Squarzoni C, Delacourt C, Allemand P. Nine years of spatial and temporal evolution of the La Valette Landslide observed By SAR interferometry[J].Engineering Geology,2003,68(1-2):53-66.

Wang G J，Xie M W，Qiu C, et al. Application of D-INSAR technique to landslide monitoring [J]. Rock and Soil Mechanics，2010，31(4)：1337-1344.

Wang L W. Indentification of landslide displacement in alpine valley region based on D-InSAR data analysis [D]. University of Science and Technology Beijing, 2015.

Wang T. Time series InSAR analysis over the three gorges region: Technique and Applications [D]. Wuhan University, 2010.

Xia Y, Kaufmann H, Guo XF. Landslide monitoring in the three gorges area using d-insar and corner reflectors[J]. PE& RS, Photogrammetric Engineering & Remote Sensing,2004,70(10):1167-1172.

Zhang J L, Vernon h, Singhro Y. Application of differential interfer ometric sar to the jiaju landslide in Sichuan, China[J]. Journal of Chengdu University of Technology(Science & Technology Edition)，2010,37(5)：554-557.

Zhang Y. Detecting ground deformation and investigating landslides using InSAR technique——taking middle reach of bailong rive r basin as an example[D]. Lanzhou University, 2018.

Zhao C, Kang Y, Zhang Q, et al. Landslide Identification and Monitoring along the Jinsha River Catchment (Wudongde Reservoir Area), China, Using the In SAR Method[J]. Remote Sensing, 2018, 10(7):993.